AGU Advances

Supporting Information for

Temperature and Hydrologic Cycle Constraints on Snowball Earth Environments

T. J. Mackey[1], A. B. Jost[1], J. R. Creveling[2], and K. D. Bergmann[1]

[1]Massachusetts Institute of Technology, Department of Earth, Atmospheric, and Planetary Sciences. [2]Oregon State University, College of Earth, Ocean, and Atmospheric Sciences.

Contents of this file

Additional Supporting Information (Files uploaded separately)

Introduction

This supporting information includes supplemental text (S1–S3) on the analytical methods followed for the study. Methods are paired with Tables S1 and S2, which provide the raw and processed isotopic data underpinning the study; raw isotopic data (Table S2) is also submitted to EarthChem database and includes the analytical information for all standards and unknowns used in generating clumped isotope reconstructions. Figure S1 and Table S2 are uploaded separately as a PDF and an Excel workbook (.xlsx), respectively. The full results of XRD analysis are listed in Table S3, following the methods in the main manuscript text. Supplemental Figures S1–S5 provide additional context on sampling sites analyzed in this study (Figures S1and S2), petrographic textures referenced in the text (Figure S3), and visualization of geochemical data sets that complement the figures in the main manuscript text (Figure S4 and S5).

Text S1. Clumped isotope analytical methods

Clumped isotope analyses were carried out on the Bergmann Lab Nu Perspective IRMS with an interfaced NuCarb autosampler held at 70°C. All carbonates were converted to CO_2 with injection of 150 μl of concentrated H_3PO_4 (1.94–1.95 g/cm^3) into the evacuated sample vial. Acidification progressed for 600 sec in the closed vial, followed by continuing reaction for

an additional 600 sec while freezing onto a -160 °C cold finger for a total reaction time of 1200 sec. This two-step digestion prevented aspiration of bubbles and associated acid residue into the autosampler valves (Nu Instruments, pers. comm.). Recent work has indicated that prolonged interactions between water vapor originating from H_3PO_4 and evolved CO_2 can affect Δ_{47} values (Swart et al., 2019). The small volume of concentrated H_3PO_4 injected and short length of exposure of CO_2 to acid-sourced water vapor are insufficient to impact the primary CO_2 Δ_{47} values. Following carbonate acidification, evolved CO_2 was purified with a cold finger water trap (-60 °C) and passive passage through a -30°C passive porapak trap (1/4" inner diameter tube filled with 0.4 g 50-80 mesh PorapakQ bracketed by silver wool) to freeze onto a second cold finger. Evolved CO_2 was subsequently transferred to a third cold finger in a microvolume and warmed to room temperature before having the pressure balanced by beam size on the reference side. Both sample and reference side microvolumes depleted together in the course of analysis. The resulting beam intensities were collected in three blocks with 20 cycles each of 20s integration. Initial voltage was 8–20 V on the m/z 44 beam for standard and unknown analyses, and this depleted by approximately 50% through analysis.

The NuCarb is equipped with a 50-vial carousel, which is analyzed over approximately 72 hours. Laboratory protocols for organization of standards to unknowns within a run changed in the course of this study (6/2017–11/2018). Throughout all analyses, four ETH standards were used to transfer values to VPDB and Carbon Dioxide Equilibrium Scale (CDES) (Dennis et al., 2011); $\delta^{13}C$, $\delta^{18}O$ and Δ_{47} values for ETH standards were taken from Bernasconi et al. (2018). Queues were planned for >18 ETH standards run alongside in house standards and <23 unknowns prior to 2/2018, and after this point the format was standardized to 22 ETH standards alongside in house standards and <25 unknowns. Shorter runs exceeded these standard:unknown ratio. In all cases, replicates for unknowns were dispersed throughout a run queue. Analytical failures due to autosampler malfunction or failure of standards and unknowns for data quality screening (Text S2) led to some differences between planned standard:unknown distributions and actual analyses. The full list of standards and unknowns run in the study is available in Table S2.

Text S2.
All samples were screening for CO_2 volume and yield using the measured carbonate mass and pressure transducer readings of CO_2 after passage through the porapak trap and cryogenic purification. Analyses with CO_2 pressures less than the equivalent of 250–300 μg of carbonate were excluded from this study.

Both standard and unknown replicates were screened for consistency within the cycles of a single analysis. In 103/1241 analyses (standards and unknowns), anomalous voltage spikes were present in cycles of specific analyses. Spikes were interpreted as instrumental errors related to reductions in the backing pressure of the dual inlet changeover block and possible arcing in the source. Spikes were clear outliers in the cycles of a given analysis, and were screened by disabling individual cycle Δ_{47} values outliers >3 standard deviations from the mean of the three analytical blocks if the analysis standard deviation for Δ_{47} values exceeded 0.05‰. Analyses were disabled if ≥10 cycles out of 60 were >3 standard deviations from the analysis mean (n = 5) or if removal of outliers did not reduce the standard deviation to less than 0.05‰ (n = 14). In the 84 analyses corrected by screening in this study, an average of

4/60 cycles were disabled, taking the average standard deviation across analysis blocks from 0.09 to 0.03‰.

Text S3.

An acid fractionation factor of 0.062‰ (Defliese et al., 2015; Müller et al., 2017) was used to convert our raw Δ_{47} data analyzed at 70°C to the 25°C Carbon Dioxide Equilibrium Scale (CDES) (Dennis et al., 2011). All measurements were translated to the VPDB and CDES reference frames using ETH standard values from Bernasconi et al. (2018). The temperature calibrations of Bernasconi et al. (2018) were also used for calculation of all Δ_{47} temperatures: $\Delta_{47} = 0.0449 \cdot \frac{10^6}{T^2} + 0.167$. We used this temperature calibration for both calcites and dolomites, given the findings of Petersen et al. (2019) that temperature reconstructions for consistent clumped isotope behavior for these mineralogies in their reprocessed interlaboratory comparison. These results are consistent with other interlab comparison studies (Bonifacie et al., 2017). The recent protodolomite thermometer of Müller et al. (2019) yields temperatures 6–14° C warmer than our preferred temperature calibration from Bernasconi et al. (2018). Non-glacial samples in our data set are more sensitive to the recalculations of this thermometer than glacial dolomites, increasing the 95% CL difference between the glacial and non-glacial dolomites from 16–36°C to 19–41°C. Our interpretations of partial preservation of changing climatic conditions are not impacted by the specific dolomite temperature calibration used.

Figure S1. Compilation of drill sites for clumped isotope analysis and microvolume sites from stratified diamictite slab; scale bar demarcations are millimeters. Data for each drill site are listed in Table S1. (File uploaded separately)
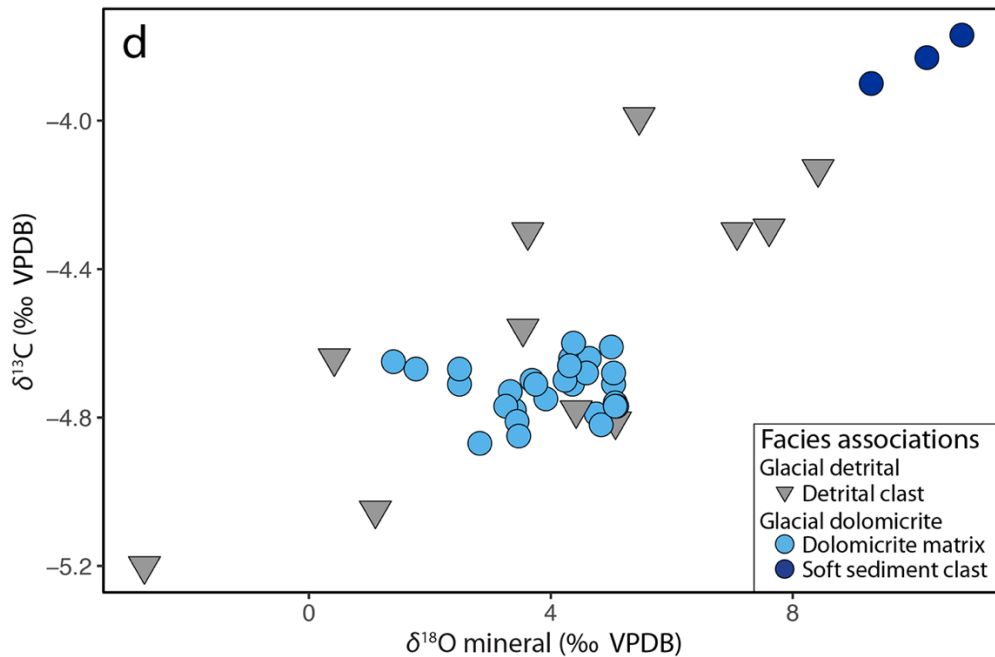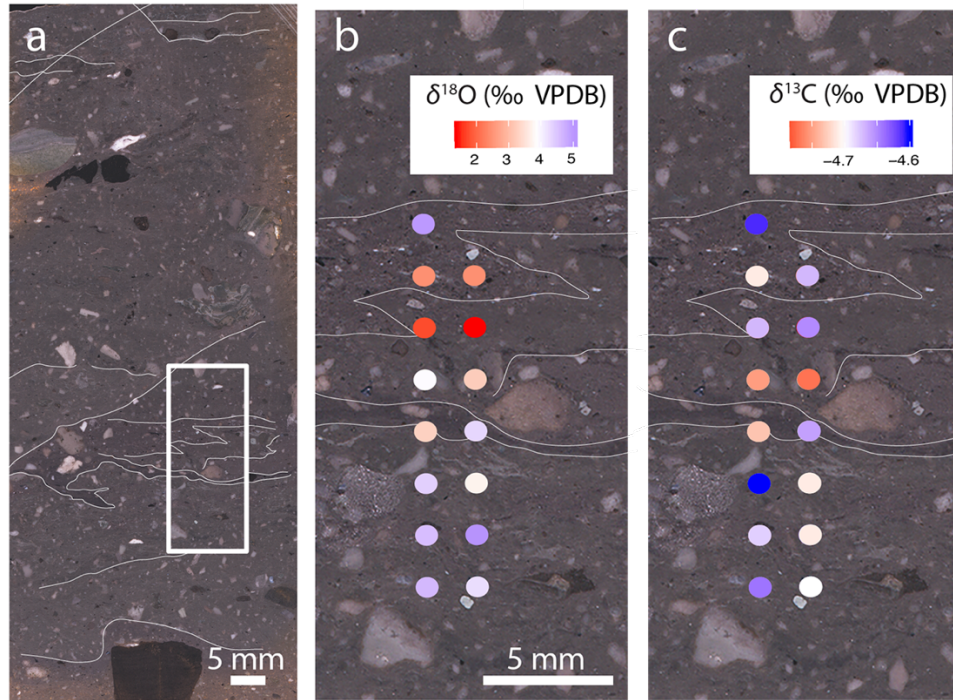

Figure S2. Microvolume analyses of stratified diamictite sample (PD5-78) $\delta^{13}C$ and $\delta^{18}O$. a) Polished slab with stratification outlined. Irregular layering is interpreted as localized glaciotectonism. b and c) Inset area from (a) with $\delta^{18}O$ (b) and $\delta^{13}C$ (c) sampling spots targeting

dolomicrite matrix across stratified layers. d) Cross plot of microvolume analyses from the PD5-78 slab. All drilled locations for this slab are presented in Figure S1.
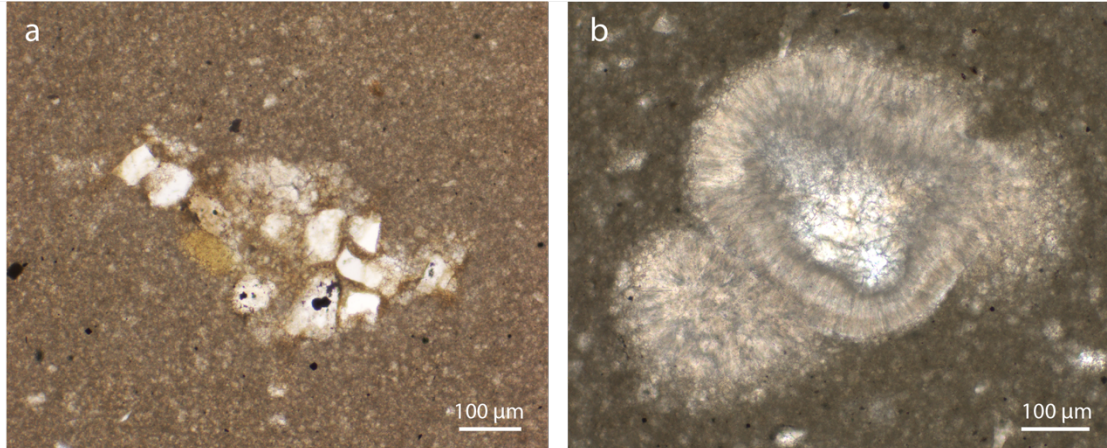

Figure S3. Supplemental petrographic attributes of Petrovbreen Member stratified diamictite referenced in the main text. a) Aggregate of siliciclastic grains in dolomicrite matrix interpreted as a till pellet. b) Carbonate grain with circumgranular sparry rims consistent with in situ precipitation (c.f. Fairchild et al., 2004).
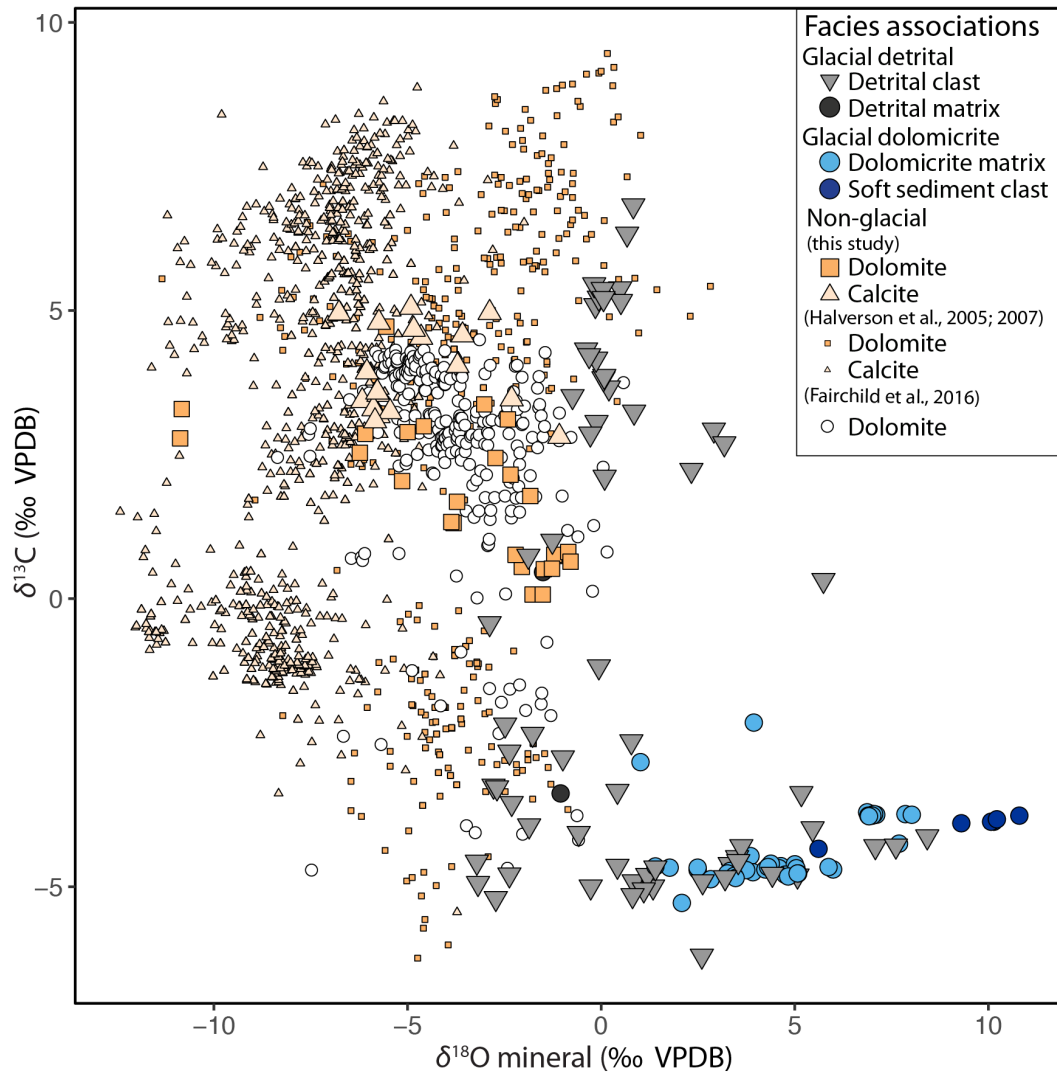
Figure S4. Cross plot of carbonate δ¹³C and δ¹⁸O values from the Tonian–
Cryogenian in NE Svalbard, as in Figure 3 of the main text, but with the addition of pre-glacial
Akademikerbreen Formation carbonates from Halverson et al. (2005; 2007) and interglacial
dolomite from the MacDonaldryggen Formation (Fairchild et al., 2016).

Table S1. Summary of data collected in this study including stratigraphic context, mean crystal size, isotope results, and notes. (File uploaded separately)

Table S2. Full report of unknown and standard clumped isotope replicate results used in compilation of summary data. Table to be formatted for EarthChem and submitted upon manuscript acceptance. (File uploaded separately)

Table S3. Summary of XRD results. Approximate mineral percent quantities are provided where available; if no percentages provided, the mineral order signifies order of abundance.

Sample	mineral 1	mineral 2	mineral 3	mineral 4	mineral 5
PD5 0.5 A	dolomite				
	100%				
PD5 2.75 A	dolomite				
	100%				
PD5 16.0 A	calcite	quartz			
	88%	22%			
PD5 30.8 A	dolomite	quartz	clinochlore	albite	
	n/a	n/a	n/a	n/a	
PD5 35.0 A-A	dolomite	quartz	albite		
	47%	37%	16%		
PD5 36.0	dolomite	albite	quartz		
	50%	29%	21%		
PD5 38.0 B	albite	dolomite	quartz		
	44%	34%	22%		
PD5 40.9 A	quartz	pyrite	dolomite	goethite	albite
	n/a	n/a	n/a	n/a	n/a
PD5 42.2 A	dolomite	quartz	pyrite	clinochlore	
	n/a	n/a	n/a	n/a	
PD5 31.3 A	quartz	dolomite	albite	clinochlore	
	n/a	n/a	n/a	n/a	

PD5 45.0 A	dolomite	albite	quartz		
	62%	19%	19%		
PD5 49.5 A	quartz	dolomite	clinochlore		
	n/a	n/a	n/a		
PD5 76.9 a A	dolomite	quartz	clinochlore		
	n/a	n/a	n/a		
PD5 78 A	dolomite	quartz	clinochlore	cristobolite?	albite
	n/a	n/a	n/a	n/a	n/a
PD5 78 B	quartz	dolomite	clinochlore	kaolinite	
	n/a	n/a	n/a	n/a	
PD5 79 C DS1	dolomite	quartz	clinochlore		
	n/a	n/a	n/a		
PD5 79 B DS2	dolomite				
	100%				
F6975 A	dolomite	quartz			
	73%	27%			
PD5 45 B	dolomite	pyrolusite			
	95%	5%			
PD5 78 C	quartz	dolomite	albite	clinochlore	
	n/a	n/a	n/a	n/a	
PD5 78 D	quartz	dolomite	albite	clinochlore	
	n/a	n/a	n/a	n/a	
PD5 27.7 A	quartz	dolomite	calcite	albite	pyrite
	n/a	n/a	n/a	n/a	n/a

PD5 38.0 C	dolomite	quartz	albite		
	46%	44%	11%		